Molecular Microbiology (2013) 88(1), 189–202 ■
doi:10.1111/mmi.12178
First published online 6 March 2013

Telomeric gene deletion and intrachromosomal amplification in antimony-resistant *Leishmania*

Angana Mukherjee,[1†] Sébastien Boisvert,[1] Rubens Lima do Monte-Neto,[1] Adriano C. Coelho,[1] Frederic Raymond,[1] Rita Mukhopadhyay,[2] Jacques Corbeil[1] and Marc Ouellette[1,*]

[1]*Centre de Recherche en Infectiologie, Université Laval, Québec, Canada, G1V 4G2.*

[2]*Department of Molecular Microbiology and Infectious Diseases, Florida International University, Herbert Wertheim College of Medicine, Miami, FL 33199, USA.*

Summary

Antimonials are still the mainstay of treatment against leishmaniasis but drug resistance is increasing. We carried out short read next-generation sequencing (NGS) and comparative genomic hybridization (CGH) of three independent *Leishmania major* antimony-resistant mutants. Copy number variations were consistently detected with both NGS and CGH. A major attribute of antimony resistance was a novel terminal deletion of variable length (67 kb to 204 kb) of the polyploid chromosome 31 in the three mutants. Terminal deletions in two mutants occurred at the level of inverted repeated sequences. The *AQP1* gene coding for an aquaglyceroporin was part of the deleted region and its transfection into resistant mutants reverted resistance to SbIII. We also highlighted an intrachromosomal amplification of a subtelomeric locus on chromosome 34 in one mutant. This region encoded for ascorbate-dependent peroxidase (APX) and glucose-6-phosphate dehydrogenase (G6PDH). Overexpression of these genes in revertant backgrounds demonstrated resistance to SbIII and protection from reactive oxygen species (ROS). Generation of a G6PDH null mutant in one revertant exhibited SbIII sensitivity and a decreased protection of ROS. Our genomic analyses and functional validation highlighted novel genomic rearrangements, functionally important resistant loci and the implication of new genes in antimony resistance in *Leishmania*.

Accepted 6 February, 2013. *For correspondence. E-mail Marc.Ouellette@crchul.ulaval.ca; Tel. (+1) 418 656 4141#48184; Fax (+1) 418 654 2715. †Present address: Department of Immunology and Infectious Diseases, Harvard School of Public Health, Boston, MA, USA.

Introduction

Leishmaniasis is caused by a protozoan parasite that affects 12–15 million people with 1.5 million new cases annually (Alvar *et al.*, 2012). There is no human vaccine against this disease (Palatnik-de-Sousa, 2008) and drugs containing pentavalent antimony (SbV) have served as a gold standard of antileishmanials for over 60 years, although their use is compromised in several endemic regions due to widespread treatment failure attributed to antimony-resistant parasites (Lira *et al.*, 1999; Sundar, 2001). The alkylphospholipid compound miltefosine, liposomal amphotericin B and paromomycin are effective alternative therapies for Old World leishmaniasis, despite higher costs (Jha *et al.*, 1999). However, in many parts of the world antimonials remain the first lines of drugs against all forms of leishmaniasis.

Current evidences from *in vitro* studies indicate that SbV is a pro-drug which is reduced to the active trivalent form (SbIII) in the host macrophage and in the intracellular *Leishmania* amastigote (Roberts *et al.*, 1995; Sereno *et al.*, 1998; Ephros *et al.*, 1999; Shaked-Mishan *et al.*, 2001). Some studies suggest that SbV can also activate macrophages (Mookerjee Basu *et al.*, 2006). The routes of uptake of SbV and SbIII into *Leishmania* are different (Brochu *et al.*, 2003), and although the former remains unidentified, SbIII is imported by a specific aquaglyceroporin (AQP1) (Gourbal *et al.*, 2004) and reduced expression of AQP1 was associated with SbIII resistance (Gourbal *et al.*, 2004; Marquis *et al.*, 2005). Although the mechanism of action of antimony is still unclear, SbIII induces apoptotic like features including accumulation of reactive oxygen species (ROS), drop in mitochondrial potential, genomic DNA degradation and increase in intracellular Ca^{2+} (Sereno *et al.*, 2001; Lee *et al.*, 2002; Sudhandiran and Shaha, 2003; Vergnes *et al.*, 2007; Moreira *et al.*, 2011). In addition, antimony-resistant phenotype of clinical isolates was accompanied by a decreased propensity to undergo apoptosis following exposure to SbIII (Vergnes *et al.*, 2007). In parallel, enhanced antioxidant defences have been reported to provide clinical resistance to antimonials (Wyllie *et al.*, 2008; 2010).

Resistance to antimony often involves detoxification of SbIII via conjugation to the unique parasitic dithiol

trypanothione (T[SH]2), and subsequent sequestration of the metal–thiol conjugate into vesicular membranes of *Leishmania* by a specific ABC protein transporter (MRPA) (Grondin *et al*., 1997; Haimeur *et al*., 2000; Legare *et al*., 2001). Amplification of genes involved in these pathways is often observed in drug-resistant mutants. Gene amplification usually occurs as extrachromosomal elements where 20–70 kb chromosomal regions recombine at the level of direct or inverted repeated sequences and generate extrachromosomal amplifiable elements (Beverley, 1991; Ouellette *et al*., 1991; Grondin *et al*., 1993; 1996). In addition to amplification of specific loci, chromosomal aneuploidies were related to SbIII resistance (Leprohon *et al*., 2009) and an extensive variation in chromosome copy number was observed in sensitive and resistant clinical isolates although the link to resistance was unclear (Downing *et al*., 2011). Some of the factors highlighted in *in vitro* studies were also shown to be implicated in natural antimony resistance in the field (Decuypere *et al*., 2005; Mittal *et al*., 2007; Mukherjee *et al*., 2007; Mandal *et al*., 2010; Kumar *et al*., 2012). Another recent study demonstrated that the molecular changes associated with antimonial resistance in natural *Leishmania* populations depend on their genetic background (Decuypere *et al*., 2012).

Whole-genome analysis by next-generation sequencing (NGS) (Downing *et al*., 2011; Rogers *et al*., 2011; Coelho *et al*., 2012) and comparative genomic hybridization (CGH) (Ubeda *et al*., 2008; Leprohon *et al*., 2009) have proven to be useful in highlighting gene amplification events and aneuploidy in resistant isolates. In this study we used a combination of these techniques to find novel gene rearrangements and new genes involved in antimony resistance in *Leishmania major*.

Results

Characterization of antimonial resistance phenotype in L. major

Three independent *L. major* mutants (LmjFSbIII1000.3, LmjFSbIII1000.4 and LmjFSbIII1000.5) were selected in a step by step manner for antimony resistance. The EC_{50} of the clonal wild-type (WT) sensitive line of *L. major* Friedlin strain was close to 2 μM, while those clones derived from the mutants were higher than 1 mM (Table 1). The stability of the resistance phenotype was tested by subculturing the promastigotes for 30 passages in the absence of SbIII. Resistance in LmjFSbIII1000.4 was found to be stable, while the phenotype was less stable in LmjFSbIII1000.3 and LmjFSbIII1000.5 with an EC_{50} of 103 and 68 μM respectively. However, these two revertants remained at least 25-fold more resistant than the WT isogenic line (Table 1).

Table 1. EC_{50} of SbIII in *Leishmania* cells.

Strain	EC_{50} (μM)
LmjFWT	2 ± 0.4
LmjFSbIII1000.3	> 1000
LmjFSbIII1000.4	> 1000
LmjFSbIII1000.5	> 1000
LmjFSbIII1000.3 Rev	103 ± 26.5
LmjFSbIII1000.4 Rev	782 ± 59.2
LmjFSbIII1000.5 Rev	68 ± 10.5
LmjFSbIII1000.3 + pSPBT1YNEOα	> 1000
LmjFSbIII1000.4 + pSPBT1YNEOα	> 1000
LmjFSbIII1000.5 + pSPBT1YNEOα	> 1000
LmjFSbIII1000.3 + pSPBT1YNEOαAQP1	22 ± 2.5
LmjFSbIII1000.4 + pSPBT1YNEOαAQP1	49 ± 5.8
LmjFSbIII1000.5 + pSPBT1YNEOαAQP1	21 ± 3.2
LmjFWT + pSPαNEOαAPX	2 ± 0.6
LmjFWT + pSPαNEOαG6PDH	2.3 ± 0.6
LmjFSbIII1000.3 Rev + pSPαNEOα	90 ± 13.5
LmjFSbIII1000.3 Rev + pSPαNEOαAPX	241 ± 47.9
LmjFSbIII1000.3 Rev + pSPαNEOαG6PDH	181 ± 25.4
LmjFSbIII1000.5 Rev + pSPαNEOα	50 ± 1.4
LmjFSbIII1000.5 Rev + pSPαNEOαAPX	147 ± 3.2
LmjFSbIII1000.3 Rev + pSPαNEOαG6PDH	96 ± 9.3

Antimony susceptibility in *L. major* SbIII-resistant mutants, revertants and transfectants. Growth of promastigotes was monitored at 72 h in the presence of various concentrations of SbIII by measuring their OD at 600 nm. The average of at least three independent experiments is shown.

CGH and NGS of antimony-resistant clonal mutants

We undertook a CGH study using a full-genome array (Ubeda *et al*., 2008) with the clonal resistant lines and parental isogenic sensitive line to measure changes in copy number. The differential hybridization data of each mutant with respect to the WT is represented in a chromosome by chromosome fashion in Fig. 1A. The red and green bars indicate the genes in higher and lower copy number respectively when compared with the WT clonal population. *L. major* Friedlin (LmjF) WT and drug-resistant clones were also analysed by NGS using Illumina Genome Analyser IIx with 76 bp single-end reads. We obtained a total of 30 083 681; 30 424 236; 29 137 023 and 34 210 773 reads for the WT, LmjFSbIII1000.3, LmjFSbIII1000.4 and LmjFSbIII1000.5 strains respectively leading to an average genome coverage of 50-fold for all the strains sequenced. A circular representation of CNV across chromosomes generated by the Circos software (Krzywinski *et al*., 2009) indicated different read depths between WT and resistant lines (Fig. 1B). Average read depth for most of the chromosomes in WT (including chromosome 34) was 50. Analysis of read depth of all chromosomes in comparison with chromosome 34 in WT (known to be disomic through gene inactivation experiments; Coelho *et al*., 2012 and see below) suggested that most chromosomes are disomic but chromosomes 1, 11, 20, 23 are trisomic, chromosome 5, tetrasomic and chromosome 31 at least hexasomic (Fig. 1B). In all *Leishma-*

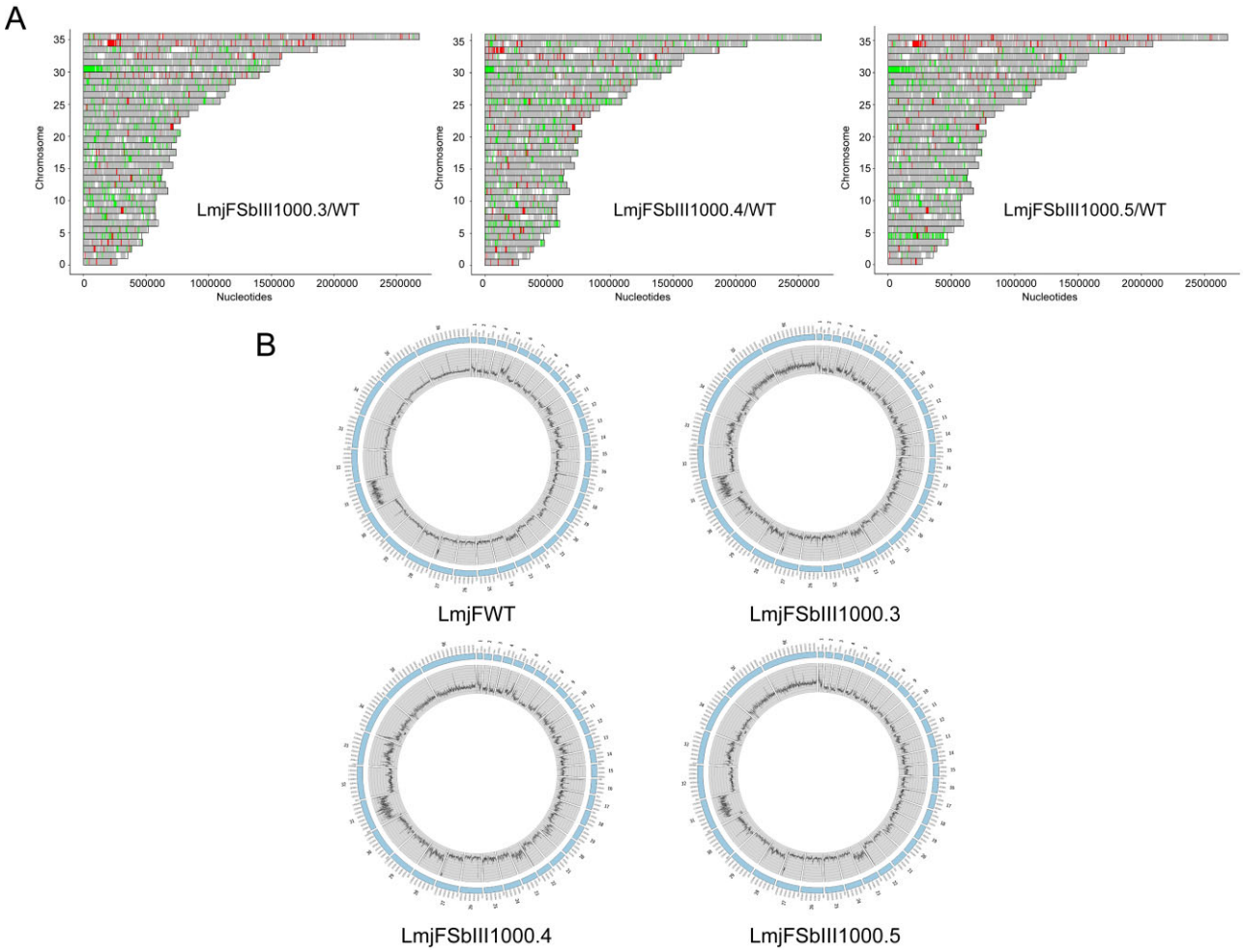

Fig. 1. Comparative genomic hybridization and next-generation sequencing of *L. major* SbIII-resistant mutants.
A. Chromosome maps of the 36 chromosomes of *L. major* LmjFSbIII1000.3/WT, LmjFSbIII1000.4/WT and LmjFSbIII1000.5/WT were generated from CGH data. Genomic DNA from clonal WT or mutants were differentially hybridized to whole-genome DNA microarrays. Green bars represent genes with a lower copy number and red bars are genes with higher copy number in the mutants compared with WT. Grey features indicate unchanged copy number.
B. Circular representation of whole-genome read counts by Circos. Whole genome of clonal LmjFWT and mutants were sequenced by Illumina with 76 bp single end reads. Outer circle represents the 36 chromosomes and the inner circle represents read counts along the length of each chromosome.

nia species characterized so far, including clinical isolates, chromosome 31 has been reported to be polyploid (Downing *et al.*, 2011; Rogers *et al.*, 2011; Coelho *et al.*, 2012). Read depth ratio from NGS and CGH of all the chromosomes of the three mutants were compared with WT and are summarized in supplemental Table S1. A strong association was observed in chromosomal aneuploidies between CGH and NGS (Fig. 1 and Table S1). Average read depth ratio predicted changes in chromosomal copy number in specific mutants. These changes translated either in a decrease in 'somy' such as chromosome 5 and 11 in the three mutants (Fig. S1A and Table S1), or in an increase in 'somy' such as chromosomes 15, 30, 35 and 36 in LmjFSbIII1000.3 and LmjFSbIII1000.5 (Fig. S1B and Table S1).

Terminal deletion of subtelomeric locus on chromosome 31

CGH maps and read depth coverage from NGS in the three mutants suggested a terminal deletion of variable length of at least four copies of chromosome 31 in all the three mutants (Fig. 2A and B). A *L. major* miltefosine mutant, LmjFMF80.3 (Coelho *et al.*, 2012) normalized with LmjFWT is shown as a control (Fig. 2A). Upon analysing the sequencing reads in that deleted subtelomeric region in LmjFSbIII1000.4, we observed that the break region was between 67 and 68 kb on chromosome 31 (Fig. 2B, middle panel). A similar analysis of subtelomeric sequencing reads of LmjFSbIII1000.3, indicated a heterogeneous genotype (Fig. 2B, left panel) with one break

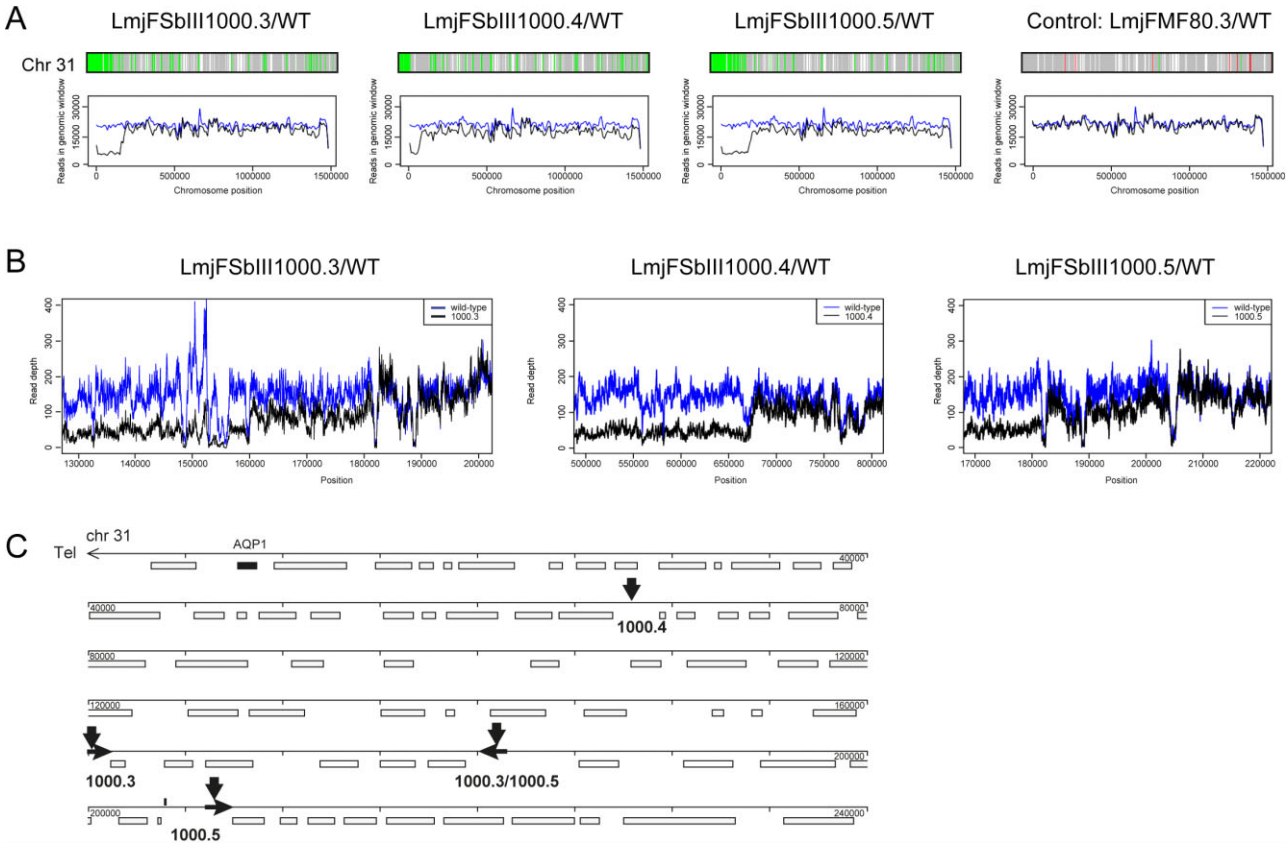

Fig. 2. Terminal deletion of chromosome 31 in *L. major*-resistant mutants.
A. Chromosome maps and sequencing reads of chromosome 31 in *L. major* WT and resistant mutants obtained from CGH and NGS. To provide a bird's view on the copy numbers, aligned reads were grouped in genomic windows of 10 000 nucleotides (Chiang *et al.*, 2009). A *L. major* miltefosine mutant MF80.3 (Coelho *et al.*, 2012) normalized with LmjFWT is shown as a control. Green bars and red bars are genes with lower and higher copy number compared with WT respectively. Blue lines: sequencing reads from LmjFWT; black line: reads from resistant mutants.
B. Sequencing reads at the break point regions of chromosome 31; blue: LmjFWT; black: mutants. Alignments were converted to read depth for each chromosome position.
C. Subtelomeric region of chromosome 31 demonstrating the break point regions (vertical arrows) in LmjFSbIII1000.3, LmjFSbIII1000.4 and LmjFSbIII1000.5 and the presence of inverted repeated sequences (horizontal arrows) at the break points. Two break points were observed for each of LmjFSbIII1000.3 and LmjFSbIII1000.5. Each line is 40 kb and boxes below the lines represent genes. *AQP1* (*LmjF31.0020*) is highlighted in black.

region estimated at 181.8–182.4 kb and another break predicted at 159.4–160.1 kb in a smaller subclonal population (Fig. 2B left panel). It is intriguing that the sequencing reads in the mutant and WT at both these break regions dropped to almost zero, after which the mutant at 181.8–182.4 kb gained back the same read depth as WT (Fig. 2B, left panel). LmjFSbIII1000.5 showed an even more pronounced heterogeneous profile in terms of the sequencing reads of subtelomeric locus on chromosome 31 (Fig. 2B, right panel). Indeed, one break point occurred at 204–205 kb from the telomeric end, another break occurred, as suggested from sequence read depths, at 181.8–182.4 kb from the chromosomal end (Fig. 2B, right panel). Upon careful inspection of these breaks, we observed the presence of inverted repeated sequences of 588 bp at positions 159 528–160 122, 181 727–182 309 and 204 322–204 904 bp (Fig. 2C and Table S2). The mapping revealed that three of the different chromosomal breaks deduced from NGS occurred at the level of these inverted repeated sequences.

To validate the sequencing data and the extent of terminal deletion in these mutants, we digested intact chromosomes in agarose blocks with FseI, an enzyme that cuts at 250 kb in WT from one telomeric end (Fig. 3A). In terminally deleted loci of the mutants, shorter fragments of 70 kb, 180 kb and 50 kb in LmjFSbIII1000.3, LmjFSbIII1000.4 and LmjFSbIII1000.5 respectively should be observed along with the WT 250 kb fragment (Fig. 3A), when hybridized with *LmjF.31.0690*, a gene distal to all the break points and proximal to FseI site. Pulsed field gel electrophoresis (PFGE) of these digested chromosomes was performed and hybridization with *LmjF.31.0690* con-

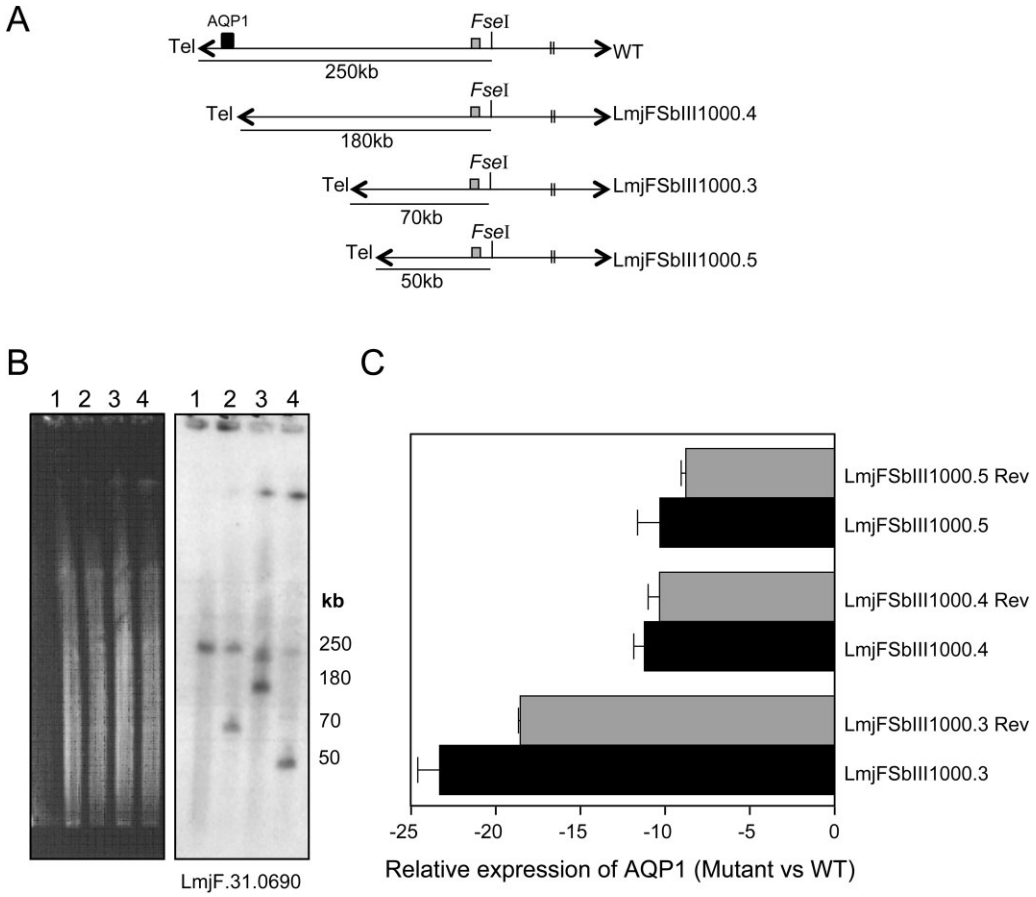

Fig. 3. Validation of terminal deletion of chromosome 31 and *AQP1* expression in *L. major* SbIII-resistant mutants.
A. Schematic diagram of chromosome 31 in *L. major* WT and the mutants. The FseI sites and the sizes of the terminally deleted chromosomes are indicated. The grey box represents the probe from *LmjF31.0690*.
B. Agarose blocks containing total DNA were digested with FseI and DNA was separated in the range of 50 kb to 500 kb (left). Southern blot was hybridized with *LmjF31.0690* probe. 1, LmjFWT; 2, LmjFSbIII1000.3; 3, LmjFSbIII1000.4 and 4, LmjFSbIII1000.5.
C. *AQP1* RNA expression in SbIII-resistant mutants and their corresponding revertants by quantitative real-time RT-PCR. The *AQP1* RNA expression ratios of resistant mutants to WT were measured and normalized with *GAPDH* expression. The values are the mean of three independent experiments each performed with three biological RNA preparations.

firmed the sizes of the deleted fragments (Fig. 3B). In LmjFSbIII1000.5, we also observed a faint band in the 70–75 kb range, suggesting that another small sub population existed as discussed above (Fig. 3B, lane 4). The hybridization intensity of the 250 kb band in the mutants was usually fainter suggesting that the deletion occurred in several of the copies of chromosome 31 (Fig. 3B, lanes 2–4).

Deletion and expression levels of LmjF.31.0020 (AQP1) and SbIII susceptibility

The second gene from the telomeric end (*LmjF.31.0020*) codes for aquaglyceroporin AQP1 (Fig. 2C), which mediates SbIII transport into the parasites (Gourbal *et al.*, 2004; Marquis *et al.*, 2005). The most plausible reason for the three independent terminal deletions of chromosome 31 in the drug-resistant mutants is to reduce the copy number and expression of AQP1. We demonstrated by qRT-PCR a 10- to 22-fold reduced expression of AQP1 in the resistant mutants and their corresponding revertants when compared with WT (Fig. 3C). Transfecting an episomal vector encoding AQP1 into the mutants reduced their EC_{50} to SbIII by 20- to 50-folds (Table 1).

Subtelomeric segmental amplification of chromosome 34

We observed a subtelomeric amplification of part of chromosome 34 in LmjFSbIII1000.4 but not in the other mutants by CGH and NGS (Fig. 1 and Fig. 4A). Zooming into the sequencing reads in this part showed that amplification extends for 162 kb starting from a telomeric end to *LmjF.34.0450* (Fig. 4A). An increase of copy number of a segment close to a telomere is often an indication of a linear amplicon (Ubeda *et al.*, 2008), but this was not the

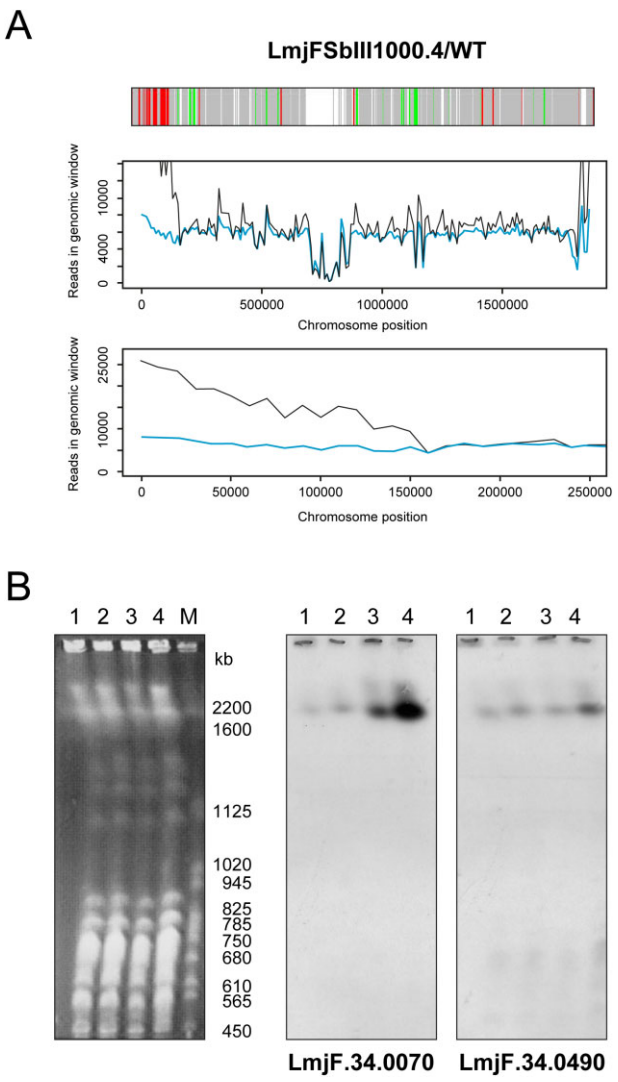

Fig. 4. Subtelomeric segmental amplification in chromosome 34 of LmjFSbIII1000.4.
A. Chromosome map and sequencing reads of chromosome 34 in LmjFSbIII1000.4 as obtained from CGH and NGS. Red and green bars are the high and low-copy-number genes respectively when compared with WT. Blue line: sequencing reads from LmjFWT; black line: reads from resistant mutant. The third panel is a zoomed version of the sequencing reads at the region of rearrangement of 162 kb from one telomeric end of chromosome 34 in LmjFSbIII1000.4.
B. PFGE was performed and chromosomes were separated between 600 kb and 1000 kb, blotted and probed with genes *LmjF.34.0070* and *LmjF.34.0490* within and outside the amplified locus respectively. Densitometric analysis revealed 2.5-fold more DNA in lane 4. 1, LmjFWT; 2, LmjFSbIII1000.3; 3, LmjFSbIII1000.4; 4, LmjFSbIII1000.4Rev; M, CHEF DNA size marker (0.225–2.2 Mb *Saccharomyces cerevisiae* chromosomal DNA).

case for LmjFSbIII1000.4 as determined by PFGE (Fig. 4B). Instead we observed that the amplified region appeared integrated on a high-molecular-weight chromosome (Fig. 4B and results not shown). A probe recognizing *LmjF.34.0070* hybridized only to a region corresponding to chromosome 34 in every strain with the hybridization signal increasing specifically in LmjFSbIII1000.4 (Fig. 4B, lane 3). This was not the case for a control probe from a gene distal to the amplification (*LmjF.34.0490*, Fig. 4B, lane 3). This amplification was stable and was not lost in cells grown for 30 passages without drug (Fig. 4B, lane 4). This observation is consistent with an intrachromosomal segmental amplification, although we cannot exclude a duplicative translocation to another high-molecular-weight chromosome. We investigated the possibility of tandem amplification by digesting intact chromosomes with AseI and probing with selected genes, spanning within (probes 1–4; Fig. 5) and outside (probes 5, 6; Fig. 5) the amplified region. The genes within the amplified segment were part of a WT band of 200 kb and of a new rearranged band at 300 kb (Fig. 5). This was not the case with probes 5 and 6. Densitometric analysis revealed that the rearranged band hybridizing to probe 1 and 2 were in two copies compared with the 200 kb wild-type band (Fig. 5) but of the same copy number than the WT band when hybridized to probe 3 and 4 (Fig. 5) suggesting a more complex rearrangement. This is also consistent with the gradual increase in reads depth as sequences are closer to the telomeres (Fig. 4A). If the rearrangement was by simple tandem amplification on one allele, hybridization with probes 5 and 6 should have also given two bands of equal intensity at 200 kb and 300 kb, but instead, a single band of 200 kb was observed (Fig. 5). The separation of AseI-digested chromosomes by PFGE followed by Southern blot hybridization with the most proximal subtelomeric genes of chromosomes 33, 34 and 35 revealed that the banding pattern was similar between wild-type and LmjFSbIII1000.4, thus excluding the possibility that rearrangement was by subtelomeric translocation (Fig. S2).

Several genes on the amplified fragment of chromosome 34 may have potential roles in SbIII resistance. We investigated two genes *LmjF.34.0070* and *LmjF.34.0080* encoding for an ascorbate-dependent peroxidase (APX) and a putative glucose-6-phosphate dehydrogenase (G6PDH) respectively. Antimonials are known to produce ROS (Mehta and Shaha, 2006; Moreira *et al.*, 2011) and both enzymes are central to the redox defence in *Leishmania* (Pal *et al.*, 2010) (Fig. S3). We cloned the APX and G6PDH genes into an episomal vector and transfected them independently in backgrounds of LmjFWT, LmjFSbIII1000.3Rev and LmjFSbIII1000.5Rev. Transfection of neither *APX* nor *G6PDH* conferred SbIII resistance in wild-type cells (Table 1). However transfection of either gene provided a two- to threefold SbIII resistance in the revertant backgrounds of LmjFSbIII1000.3 and LmjFSbIII1000.5 (Table 1). Transfection of *APX* and *G6PDH* in *Leishmania tarentolae* SbIII revertant cells also generated a four- to fivefold resistance to SbIII (results not shown). The phenotypes observed were specific to these two

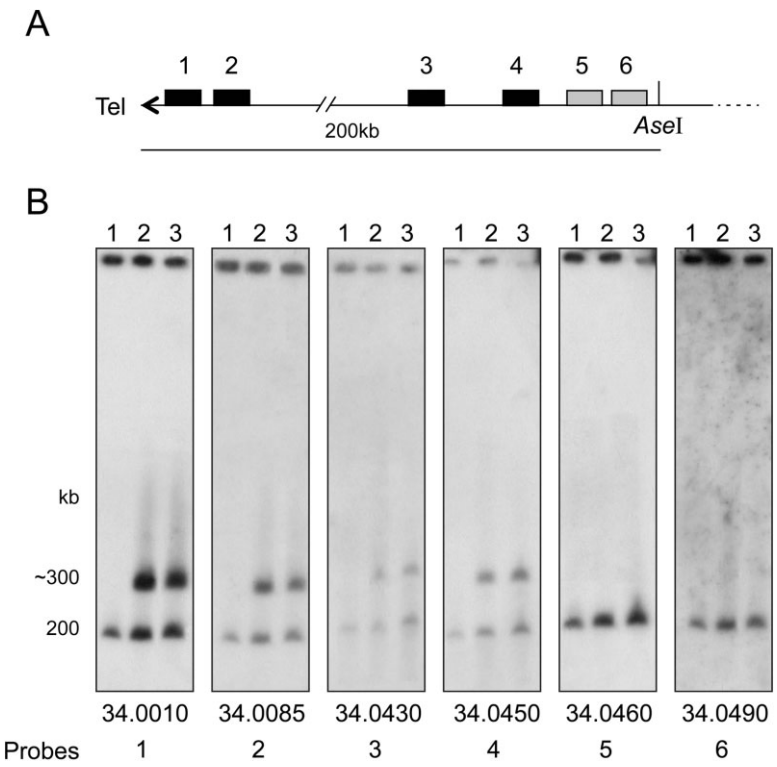

Fig. 5. Mapping of the intrachromosmal amplification in LmjFSbIII1000.4.
A. Schematic diagram of one subtelomeric locus of chromosome 34 in WT with the first AseI site shown. Black boxes depict genes part of the amplified region. Grey boxes represent genes distal to amplification and rearrangement. Gene annotation numbers are found below the blots.
B. Agarose blocks containing intact chromosomes were digested with AseI, used for PFGE and hybridized with probes from selected genes spanning within (probes 1–4) and outside (probes 5 and 6) the amplified locus. 1, LmjFWT; 2, LmjFSbIII1000.4; 3, LmjFSbIII1000.4 Rev.

genes since transfection of *LmjF.34.0350* (eukaryotic translation initiation factor 5), also part of the amplified locus of chromosome 34, in the revertant backgrounds did not generate SbIII resistance (data not shown). Revertants overexpressing APX or G6PDH were resistant to SbIII possibly because of the protection conferred by these redox enzymes against oxidative stress that SbIII is known to induce (Mehta and Shaha, 2006; Moreira *et al.*, 2011). Indeed, we observed a significant protection from ROS accumulation in APX and G6PDH overexpressors when compared with mock-transfected cells (Fig. 6). ROS accumulation was at least 1.7-fold less when APX or G6PDH overexpressors were treated with SbIII compared with their parental revertants (Fig. 6).

Since we assigned a novel role of resistance to G6PDH in a revertant background, we generated a G6PDH null mutant in the LmjFSbIII1000.3 revertant background by gene inactivation. The first and second rounds of G6PDH inactivation were by integration of neomycin phosphotransferase (*NEO*) and hygromycin phosphotransferase (*HYG*) linear cassettes respectively (Fig. 7A). Genomic DNA was isolated from clonal mutants and digested with XmnI (Fig. 7B). Upon hybridization with the probe flanking the 5′ untranslated region of *G6PDH*, we observed the 4.6 kb *NEO* band along with the 5.5 kb WT band in 1:1 ratio in the *G6PDH/NEO* single knockout cells (Fig. 7B, lane 2). In the *HYG/NEO G6PDH*$^{-/-}$ null mutant, we observed the presence of the expected 4.6 kb *NEO* and 4.8 kb *HYG* bands with the loss of the 5.5 kb WT band (Fig. 7B, lane 3).

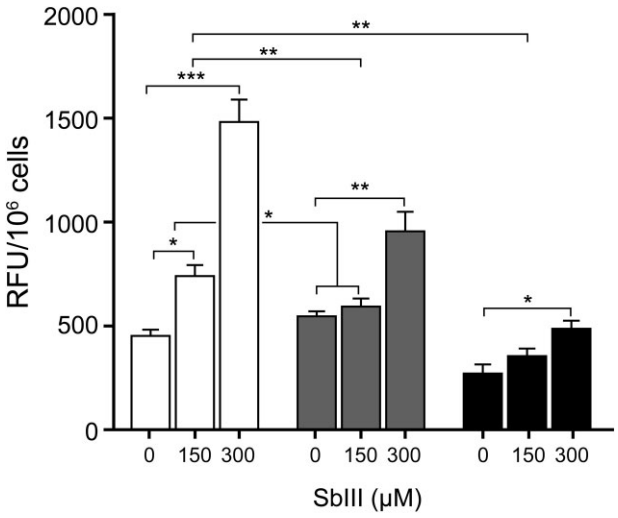

Fig. 6. Reactive oxygen species (ROS) accumulation in *Leishmania* cells. ROS was measured with 2′,7′-dichlorodihydrofluorescein diacetate (H_2DCFDA) dye whose intracellular fluorescence intensity is proportional to the level of ROS. LmjF1000.5 rev cells transfected with pSPαNEOα (white); pSPαNEOαAPX (grey); pSPαNEOαG6PDH (black). Cells from mid-log phase were either untreated (0) or treated with 150 μM or 300 μM SbIII for 24h. Cells were washed with HEPES NaCl and resuspended with H_2DCFDA and incubated at 25°C for 30 min. Fluorescence was measured at 530 nm and relative fluorescence units (RFU) were normalized to 10^6 cells. Results are mean of three biological replicates performed in triplicates. An unpaired two-tailed *t*-test was performed to compare the significance between means of different groups. $^*P < 0.05$; $^{**}P < 0.01$; $^{***}P < 0.001$.

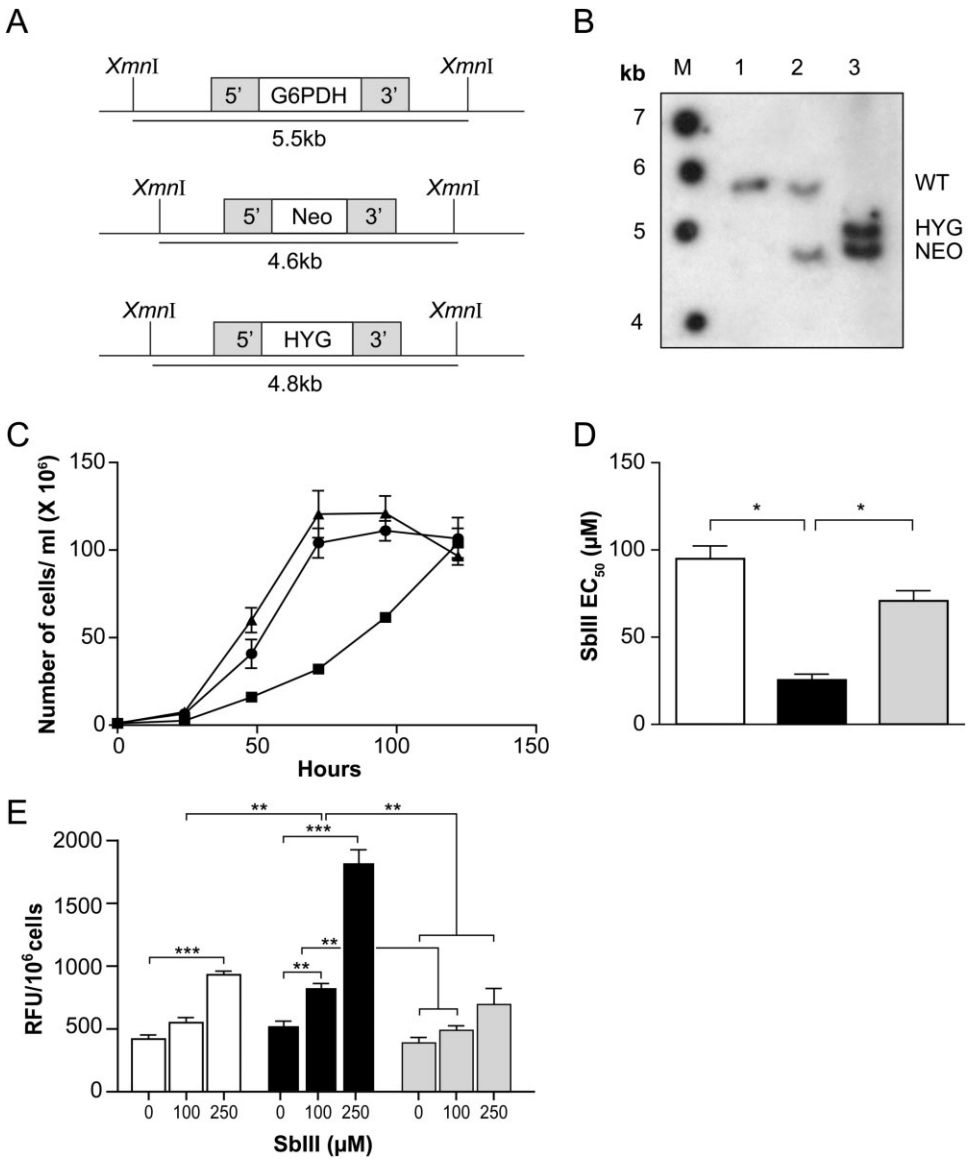

Fig. 7. Inactivation of the glucose-6-phosphate dehydrogenase (*G6PDH*) gene and its role in antimonial resistance.
A. Schematic representation of *G6PDH* (*LmjF.34.0080*) locus before and after integration of the inactivation cassette *NEO* (neomycin phosphotransferase) and HYG (hygromycin phosphotransferase) and the relevant XmnI sites.
B. Southern blot analysis with XmnI-digested genomic DNA from clonal mutants and probed with 557 bp of 5′ UTR of *G6PDH*. Molecular weights are indicated on the left. 1, LmjFSbIII1000.3Rev; 2, LmjFSbIII1000.3RevG6PDH$^{+/-}$; 3, LmjFSbIII1000.3RevG6PDH$^{-/-}$.
C. Growth retardation of G6PDH null mutants. Growth of LmjFSbIII1000.3Rev (pSPαZEOα) (●), LmjFSbIII1000.3RevG6PDH$^{-/-}$ (pSPαZEOα) (■) and LmjFSbIII1000.3RevG6PDH$^{-/-}$ (pSPαZEOαG6PDH) (▲) were monitored for 120 h by cell counting. Graph represents the average of two independent experiments.
D. LmjFSbIII1000.3Rev (pSPαZEOα) (white bar), LmjFSbIII1000.3RevG6PDH$^{-/-}$ (pSPαZEOα) (black bar) and LmjFSbIII1000.3RevG6PDH$^{-/-}$ (pSPαZEOαG6PDH) (grey bar) were tested for their SbIII susceptibility. Graph represents the mean EC_{50} of three independent experiments.
E. ROS accumulation in the mutants. LmjFSbIII1000.3Rev (pSPαZEOα) (white bar), LmjFSbIII1000.3RevG6PDH$^{-/-}$ (pSPαZEOα) (black bar) and LmjFSbIII1000.3RevG6PDH$^{-/-}$ (pSPαZEOαG6PDH) (grey bar) were either untreated (0) or treated with 100 μM or 250 μM SbIII as indicated, washed and resuspended in HEPES NaCl with H_2DCFDA and incubated at 25°C for 30 min. Fluorescence was measured at 530 nm and RFU was normalized to 10^6 cells. Results are average of three biological replicates performed in triplicates. An unpaired two-tailed *t*-test was performed to compare the significance between means of different groups. *$P < 0.05$; **$P < 0.01$; ***$P < 0.001$.

LmjFSbIII1000.3Rev *G6PDH*$^{-/-}$ transfected with an empty vector (pSPα*ZEO*α), demonstrated specific growth retardation when compared with the control parental revertant line (Fig. 7C). This growth retardation was rescued upon the add-back of an episomal construct encoding G6PDH (LmjFSbIII1000.3RevG6PDH$^{-/-}$ add-back) (Fig. 7C). The *G6PDH*$^{-/-}$ mutant cells demonstrated a significant three-fold increased sensitivity to SbIII which was complemented

in the add-back strain (Fig. 7D). The G6PDH null mutant also accumulated 1.5-fold more ROS when treated with 250 μM SbIII compared with its parental strain and this was complemented in the add-back strain (Fig. 7E).

Discussion

We carried out CGH and NGS on three independent *L. major* SbIII mutants in order to identify mutations linked to SbIII resistance. In contrast to a recent genome analysis of *L. major* miltefosine-resistant mutants (Coelho *et al*., 2012), we could not validate any single-nucleotide polymorphisms (SNPs) in coding sequences of any of the antimony-resistant mutants. Polymorphisms were mostly due to heterozygosity in the WT population. While point mutations do not seem to play a major role in antimony resistance in the strains studied, CNVs were more frequent. Indeed the chromosome structures of the mutants differed notably as inferred from both NGS and CGH where chromosomal aneuploidies, terminal deletion and intrachromosomal segmental amplification were observed in the SbIII mutants.

Chromosomal aneuploidy in *Leishmania* isolates has recently been reported using both CGH (Ubeda *et al*., 2008; Leprohon *et al*., 2009) and whole-genome sequencing (Downing *et al*., 2011; Rogers *et al*., 2011; Coelho *et al*., 2012) and our sequencing of a LmjFWT clone confirmed that within a population not all chromosomes are disomic. Chromosomes 1, 11, 20, 23 are trisomic; chromosome 5 is tetrasomic and chromosome 31 is at least hexasomic (Fig. 1). Upon induction of SbIII resistance, specific chromosomal copy number changes occurred in either one, two or three mutants (Fig. 1, Fig. S1, Table S1). In general a positive link was observed between CGH and NGS (Fig. 1, Table S1). Chromosomal aneuploidy has been observed for azole resistance in *Candida albicans* (Selmecki *et al*., 2006; Polakova *et al*., 2009) and shown to be involved in resistance but additional work will be required to test this link in *Leishmania*.

An important chromosomal aberration in the three mutants was a terminal deletion of 67 kb to 204 kb in chromosome 31, hence decreasing the copy number and expression of *AQP1* (Figs 2 and 3), the main route of entry of trivalent antimony in *Leishmania* (Gourbal *et al*., 2004). Transfection of *AQP1* in resistant mutants sensitize them to SbIII (Table 1) confirming that reducing the expression of AQP1 mediated by terminal deletion of chromosome 31 is a major mechanism of SbIII resistance in these mutants. Transfection of *AQP1* did not, however, resensitize cells to wild-type levels (Table 1) suggesting that other mechanisms are involved. Some of these putative mechanisms (e.g. change in ploidy, post-transcriptional or translational regulation) appears unstable since the revertants of mutants 3 and 5 lose resistance factors (Table 1). Future comparison of revertants and mutants may eventually lead to the identification of these additional mechanisms.

While telomere-mediated chromosome fragmentation has been used previously to induce breakage of *Leishmania* chromosomes (Tamar and Papadopoulou, 2001), this is the first example of drug induced natural terminal deletion in *Leishmania*. Terminal deletions are commonly observed in structural human chromosomal abnormalities and result in a variety of genetic syndromes (Bonaglia *et al*., 2011). Broken chromosomes are stabilized in humans by at least three mechanisms: *de novo* telomere addition mediated by telomerase (telomeric healing) (Wilkie *et al*., 1990); telomeric capture through which a terminally deleted chromosome acquires a new telomeric sequence from sister chromatid, homologous or non-homologous chromosomes (Meltzer *et al*., 1993) and generates a derivative chromosome; stabilization by break–fusion–break (BFB) cycles, generating terminal deletions and proximal inverted duplications. If the terminal deletions on chromosome 31 in *Leishmania* were by a double-strand break, the simplest mechanism to heal the breaks would be by seeding of telomeric repeats at the break point by telomerase.

The presence of repeated sequences may play a role in generation and/or stabilization of these terminal deletions. Repetitive elements like Alu, LINE, SINE, LTR are often present at break points of terminally deleted human chromosomes (Yatsenko *et al*., 2009). In this study, we observed 588 bp inverted repeated sequences at three break points out of four (Fig. 2 and Table S2) in three mutants. These inverted repeated DNA sequences may be associated in the generation and/or stabilization of terminal deletions in the SbIII mutants. Repeats are susceptible to double-strand breaks due to replication errors or formation of unusual secondary structures (Narayanan *et al*., 2006) which increases probability of rearrangement. Telomeres contain large blocks of telomere-associated repeat sequences (TAR) located just proximally to the telomeric $(TTAGGG)_n$ tandem repeats providing significant sequence homology between non-homologous chromosome ends and we identified a 11 bp sequence (GAGGGT GTCGC) in the 588 bp repeats whose reverse complement (GCGACACCCTC) is microhomologous with TAR repeats. Therefore microhomology mediated break induced replication (Hastings *et al*., 2009) may also occur after a double-strand break, end resection, homology search; strand invasion and followed by telomeric capture from any TAR sequence in a non-homologous chromosome. However, we also cannot exclude that these are interstitial deletions with a distal breakpoint located within the TAR sequences and microhomology mediated end joining. This is known as a subsidiary mechanism of double-strand break repair in trypanosomes (Glover *et al*.,

2008; 2011) and may take place between TAR and the inverted repeat at 159, 182 and 204 kb from the telomeric end, thereby generating an interstitial deletion which may look like a terminal deletion.

Gene amplification in *Leishmania* is mostly by generation of extrachromosomal circular or linear amplicons (Ouellette *et al*., 1991; Grondin *et al*., 1996; Ubeda *et al*., 2008; Leprohon *et al*., 2009) mediated by homologous direct or inverted repeated sequences (Ubeda *et al*., 2008; Leprohon *et al*., 2009). We observed a 162 kb subtelomeric chromosome 34 amplification in LmjFSbIII1000.4 which was stable and intrachromosomal (Fig. 5 and Fig. S2). The exact mechanisms by which the amplicon was formed will require further analysis but it does not appear to be by simple locus duplication (Fig. 5) or translocation to a subtelomere of another high-molecular-weight chromosome (Fig. S2). This rare event of gene amplification in *Leishmania* is stable and resistance is more stable in LmjFSbIII1000.4 compared with other mutants (Table 1) suggesting that genes involved in resistance are potentially located on this intrachromosomal amplified locus.

We investigated *LmjF.34.0070* encoding for an ascorbate-dependent peroxidase (APX) and *LmjF.34.0080* coding for glucose-6-phosphate dehydrogenase (G6PDH) since they are central in redox metabolism (Fig. S3). Increasing evidences are linking SbIII in generation of apoptotic like features in *Leishmania* (Sereno *et al*., 2001; Lee *et al*., 2002; Sudhandiran and Shaha, 2003; Vergnes *et al*., 2007; Moreira *et al*., 2011). G6PDH catalyses the committed step of pentose phosphate pathway where glucose-6-phosphate is oxidized to 6-phosphogluconolactone with the concomitant reduction of $NADP^+$ to NADPH. NADPH is an essential cofactor for enzymes that scavenge ROS (Fig. S3). Overexepression of APX and G6PDH independently in WT did not render them SbIII resistant (Table 1). However, overexpression in revertant backgrounds (LmjFSbIII1000.3Rev, LmjFSbIII1000.5Rev) generated a SbIII resistance phenotype suggesting that these proteins act in conjuction with other stable resistant factors present in revertant cells to generate SbIII resistance. This resistance could be due to the protection conferred by these redox enzymes from ROS accumulation when treated with SbIII (Fig. 6). We attempted to generate a null mutant of APX in LmjFSbIII1000.3Rev. It was possible to inactivate the first allele; but not the second allele due to rearrangements (data not shown). We succeeded in generating a null mutant of G6PDH in LmjFSbIII1000.3Rev (LmjFSbIII1000.3Rev *G6PDH*$^{-/-}$) which developed a growth retardation when grown as promastigotes. A similar phenotype was observed when *G6PDH* was knocked down in *T. brucei* suggesting its importance in growth and survival (Cordeiro *et al*., 2009). Inactivation of *G6PDH* rendered the cells susceptible to SbIII and produced significantly more ROS in response to SbIII (Fig. 7D and E).

In conclusion, our genomic work has allowed detecting novel subtelomeric terminal deletions and intrachromosomal amplification. Additionally, this study has highlighted the role of novel metabolic genes correlated to resistance and to the mode of action of antimonials involving the production of ROS.

Experimental procedures

Cell lines, culture conditions and generation of SbIII resistance

Leishmania major Friedlin MHOM/IL/81/Friedlin wild-type promastigotes were grown at 25°C in SDM-79 medium supplemented with 10% heat-inactivated fetal bovine serum and 10 μg ml^{-1} haemin. Three independent SbIII-resistant mutants; LmjFSbIII1000.3, 1000.4 and 1000.5 were selected from a cloned parental population using a stepwise selection until they were resistant to 1 mM SbIII (potassium antimony(III) tartrate). Selection started at EC_{50} values and once parasites adapted (one to three passages) the drug concentration was increased by twofold. This cycle was repeated until we obtained highly resistant mutants. The mutants were cloned on SDM agar (1% Noble Agar, Nunc) plates and one clone was chosen from each resistant mutant for further characterization. Partial revertants were obtained by culturing the resistant lines in the absence of SbIII for 30 passages. Growth curves were obtained by measuring absorbance at 600 nm as previously described (Ouellette *et al*., 1990).

DNA constructs and transfections

The pSPBT1Y*NEOαAQP1* was generated by blunt end cloning and sequencing of *LmjFAQP1* in an EcoRV site of the vector pSPBT1Y*NEOα*. The pSP72α*NEOαAPX*, pSP72α*NEOαG6PDH* constructs were generated by amplifying the respective genes from *L. major* Friedlin genomic DNA with primers containing BamHI and HindIII sites and BamH1 and XbaI sites respectively, cloning in pGEMT-easy; sequencing; followed by subcloning in pSP72α*NEOα* (Gourbal *et al*., 2004). Transfection of these plasmids were performed by electroporation as reported previously (Papadopoulou *et al*., 1992). *G6PDH* inactivation cassettes for *L. major* containing hygromycin phosphotransferase B, neomycin phosphotransferase, were constructed using a polymerase chain reaction (PCR) fusion-based strategy and transfected as described previously (Mukherjee *et al*., 2009). Briefly, two micrograms of linear fragments for transfection were obtained by PCR amplification, gel purified and transfected into promastigotes by electroporation. *L. major* recombinants were preselected initially in the presence of 50 μg ml^{-1} hygromycin or 400 μg ml^{-1} paromomycin sulphate (Sigma). After 24 h, the transfected cells were grown in the presence of higher drug concentrations and cells growing in highest drug selection (100 μg ml^{-1} hygromycin, 800 μg ml^{-1} paromomycin) were cloned. The *L. major G6PDH* was amplified from genomic DNA with primers containing XbaI and HindIII sites, cloned in pGEMT-easy,

sequenced and subcloned in pSP72α*ZEO*α (Richard *et al.*, 2004) at XbaI and HindIII sites generating the plasmid pSP72α*ZEO*α*G6PDH* and was transfected in the null mutant background for complementation. Primers used in this study for amplifying the genes *AQP1* (*LmjF.31.0020*), *G6PDH* (*LmjF.34.0080*), *APX* (*LmjF.34.0070*), *LmjF.34.0350* of *L. major* and primers for generating *G6PDH*-KO and *LmjF.34.0070*-KO (*APX*-KO) constructs are listed in Table S3.

PFGE and Southern blot analysis

For preparation of intact chromosomes or digestion of chromosomes in agarose blocks, *Leishmania* promastigotes were harvested in late log phase, washed and lysed *in situ* in 1% low melting agarose plugs and run on PFGE or digested with AseI/FseI in agarose blocks as described previously (Mukherjee *et al.*, 2011) and separated on a Bio-Rad CHEF-DR III apparatus at 5 V cm^{-1}, 120° separation angle. Genomic DNA of clones was isolated using DNAzol (Invitrogen). Digested genomic DNA or separated chromosomes were subjected to Southern blot hybridization with [α-^{32}P]-dCTP-labelled DNA according to standard protocols (Sambrook *et al.*, 1989). All probes were obtained by PCR from *L. major* genomic DNA. Densitometric analyses of Southern blots were performed using Image J and Agfa Arcus 2 scanner.

Comparative genomic hybridization

Genomic DNA was isolated from mid-log-phase promastigotes by DNAzol, followed by shearing the DNA through 22 G 1″ and 27 G ½″ needles (Becton Dickinson). Sheared DNA was digested with PvuII and MseI, purified by phenol chloroform extraction and ethanol precipitation. Four micrograms of digested DNA was labelled using Cy_5- or Cy_3-dCTP (Amersham), random hexamers (Roche) and exo$^-$ Klenow DNA polymerase (NEB). Fluorescent probes were then purified with ArrayIt columns (Telechem) and quantified. Hybridization was performed as described earlier (Ubeda *et al.*, 2008). Normalization and statistical analyses were performed in R 2.2.1 software using the LIMMA (Linear Models for Microarray Data) 2.7.3 package (Smyth and Speed, 2003; Smyth, 2004; Smyth *et al.*, 2005). Background correction was performed using the 'edwards' method; within-array normalization was done by loess and between array normalization by the Aquantile method. A threshold *P*-value of 0.05 was used. Custom R programs were used for the generation of the chromosome maps. The entire data set was deposited to GEO under the reference number Series GSE41750.

Next-generation sequencing

Genomic DNA was prepared from mid-log-phase cultures of clonal *L. major* Friedlin mutants LmjFSbIII1000.3, 1000.4, 1000.5 and LmjFWT parasites and sequenced using Illumina Genome Analyser IIx 76-nucleotide single-end reads. The genome of *L. major* (v4.0) was downloaded from TriTrypDB (Aslett *et al.*, 2010). Sequence reads from each strain were aligned to the *L. major* Friedlin reference sequence (v.4.0) (Ivens *et al.*, 2005) (http://www.tritrypdb.org) using the software MAQ (Mapping and Assembly with Quality) (Li *et al.*, 2008), bwa (v0.6.1) Smith-Waterman (Li and Durbin, 2010). The standard SAM format was used for all workflows (samtools v0.1.18) (Li *et al.*, 2009). All read counts were normalized using the total yields for each sample with respect to wild-type. A circular representation of CNV across chromosomes were generated by the Circos (v0.62.1) software (Krzywinski *et al.*, 2009). Copy number plots were also generated using a genome partition scheme based on genomic windows (Chiang *et al.*, 2009). The sequence data for *L. major* antimony-resistant mutants are available at the EMBL European Nucleotide Archive (http://www.ebi.ac.uk/ena) SRA database under the Study Accession No. ERP001534. The samples accessions are ERS056015 (for LmjFWT), ERS150563 (for LmjFSbIII1000.3), ERS150564 (for LmjFSbIII1000.4) and ERS150565 (for LmjFSbIII1000.5).

Real-time RT-PCR

First-strand cDNA was synthesized from 5 μg of RNA using Oligo dT12–18 and SuperScript II RNase H-Reverse Transcriptase (Invitrogen, Carlsbad, CA, USA) according to the manufacturer protocol. Equal amounts of cDNA were run in triplicate and amplified in 25 μl of reactions containing 1× iQ SYBRH Green Supermix (Bio-Rad, Hercules, CA, USA), 100 nM forward and reverse primers and 1 μl of cDNA target. Reactions were carried out using a rotator thermocycler Rotor Gene (RG 3000, Corbett Research, San Francisco, USA). Initially, mixtures were incubated at 95°C for 5 min and then cycled 30 times at 95°C, 60°C and 72°C for 15 s. No-template controls were used as recommended. Three technical and biological replicates were established for each reaction. The relative amount of PCR products generated from each primer set was determined based on the threshold cycle (C_T) value and the amplification efficiencies. Data were analysed using the comparative $2^{-\Delta\Delta Ct}$ method. Gene expression levels were normalized to constitutively expressed mRNA encoding glyceraldehyde-3-phosphate dehydrogenase (*GAPDH*, *LmjF.30.2970*). Primers for targeted aquaglyceroporin-encoding gene, *AQP1* (*LmjF.31.0020*) and internal gene expression control *GAPDH* were designed using Primer Quest^{SM} (http://www.idtdna.com/Scitools/Applications/Primerquest). Primer sequences are listed in Table S3.

ROS measurement

For assessing the levels of ROS, promastigotes were harvested from mid-log phase and seeded at 5×10^6 cells ml^{-1}. Cells were either left untreated or treated with different concentrations of SbIII for 24 h. After 24 h, equal number of cells (4×10^7) were harvested for ROS accumulation, washed with HEPES NaCl, resuspended in HEPES NaCl containing 25 μg ml^{-1} H_2DCFDA (Invitrogen) and incubated at 25°C for 30 min. Fluorescence was measured with a Victor fluorometer (Perkin–Elmer, Turku, Finland) at 485 nm excitation and 535 nm emission wavelengths. Cells were counted again after fluorescence measurement and RFU was normalized to 10^6 cells.

Acknowledgements

We thank Dr Philippe Leprohon for help with sequence analysis and members of the lab for critical reading of the manuscript. A.M. and A.C.C. received postdoctoral fellowship from the CIHR-STP Strategic Training programme; R.L.d.M. is supported by a Government of Canada DFAIT post-doctoral research fellowship. S.B. is recipient of a Frederick Banting and Charles Best Canada Graduate Scholarship – Doctoral Award from the Canadian Institutes for Health Research (Institute of Genetics, 200910GSD-226209-172830). J.C. and M.O. are Canada Research Chair in Medical Genomics and Antimicrobial resistance respectively. Compute infrastructure was provided by the CLUMEQ/Calcul Québec consortium, part of Compute Canada (resource allocation project: nne-790-ab). This work was supported by the Canadian Institutes of Health Research (CIHR) operating grant (13233) to M.O.

References

Alvar, J., Velez, I.D., Bern, C., Herrero, M., Desjeux, P., Cano, J., *et al*. (2012) Leishmaniasis worldwide and global estimates of its incidence. *PLoS ONE* **7:** e35671.

Aslett, M., Aurrecoechea, C., Berriman, M., Brestelli, J., Brunk, B.P., Carrington, M., *et al*. (2010) TriTrypDB: a functional genomic resource for the Trypanosomatidae. *Nucleic Acids Res* **38:** D457–D462.

Beverley, S.M. (1991) Gene amplification in *Leishmania*. *Annu Rev Microbiol* **45:** 417–444.

Bonaglia, M.C., Giorda, R., Beri, S., Agostini, C.D., Novara, F., Fichera, M., *et al*. (2011) Molecular mechanisms generating and stabilizing terminal 22q13 deletions in 44 subjects with Phelan/McDermid syndrome. *PLoS Genet* **7:** e1002173.

Brochu, C., Wang, J., Roy, G., Messier, N., Wang, X.Y., Saravia, N.G., and Ouellette, M. (2003) Antimony uptake systems in the protozoan parasite *Leishmania* and accumulation differences in antimony-resistant parasites. *Antimicrob Agents Chemother* **47:** 3073–3079.

Chiang, D.Y., Getz, G., Jaffe, D.B., O'Kelly, M.J., Zhao, X., Carter, S.L., *et al*. (2009) High-resolution mapping of copy-number alterations with massively parallel sequencing. *Nat Methods* **6:** 99–103.

Coelho, A.C., Boisvert, S., Mukherjee, A., Leprohon, P., Corbeil, J., and Ouellette, M. (2012) Multiple mutations in heterogeneous miltefosine-resistant *Leishmania major* population as determined by whole genome sequencing. *PLoS Negl Trop Dis* **6:** e1512.

Cordeiro, A.T., Thiemann, O.H., and Michels, P.A. (2009) Inhibition of *Trypanosoma brucei* glucose-6-phosphate dehydrogenase by human steroids and their effects on the viability of cultured parasites. *Bioorg Med Chem* **17:** 2483–2489.

Decuypere, S., Rijal, S., Yardley, V., Doncker, S.D., Laurent, T., Khanal, B., *et al*. (2005) Gene expression analysis of the mechanism of natural Sb(V) resistance in *Leishmania donovani* isolates from Nepal. *Antimicrob Agents Chemother* **49:** 4616–4621.

Decuypere, S., Vanaerschot, M., Brunker, K., Imamura, H., Muller, S., Khanal, B., *et al*. (2012) Molecular mechanisms of drug resistance in natural *Leishmania* populations vary with genetic background. *PLoS Negl Trop Dis* **6:** e1514.

Downing, T., Imamura, H., Decuypere, S., Clark, T.G., Coombs, G.H., Cotton, J.A., *et al*. (2011) Whole genome sequencing of multiple *Leishmania donovani* clinical isolates provides insights into population structure and mechanisms of drug resistance. *Genome Res* **21:** 2143–2156.

Ephros, M., Bitnun, A., Shaked, P., Waldman, E., and Zilberstein, D. (1999) Stage-specific activity of pentavalent antimony against *Leishmania donovani* axenic amastigotes. *Antimicrob Agents Chemother* **43:** 278–282.

Glover, L., McCulloch, R., and Horn, D. (2008) Sequence homology and microhomology dominate chromosomal double-strand break repair in African trypanosomes. *Nucleic Acids Res* **36:** 2608–2618.

Glover, L., Jun, J., and Horn, D. (2011) Microhomology-mediated deletion and gene conversion in African trypanosomes. *Nucleic Acids Res* **39:** 1372–1380.

Gourbal, B., Sonuc, N., Bhattacharjee, H., Legare, D., Sundar, S., Ouellette, M., *et al*. (2004) Drug uptake and modulation of drug resistance in *Leishmania* by an aquaglyceroporin. *J Biol Chem* **279:** 31010–31017.

Grondin, K., Papadopoulou, B., and Ouellette, M. (1993) Homologous recombination between direct repeat sequences yields P-glycoprotein containing amplicons in arsenite resistant *Leishmania*. *Nucleic Acids Res* **21:** 1895–1901.

Grondin, K., Roy, G., and Ouellette, M. (1996) Formation of extrachromosomal circular amplicons with direct or inverted duplications in drug-resistant *Leishmania tarentolae*. *Mol Cell Biol* **16:** 3587–3595.

Grondin, K., Haimeur, A., Mukhopadhyay, R., Rosen, B.P., and Ouellette, M. (1997) Co-amplification of the gamma-glutamylcysteine synthetase gene *gsh1* and of the ABC transporter gene *pgpA* in arsenite-resistant *Leishmania tarentolae*. *EMBO J* **16:** 3057–3065.

Haimeur, A., Brochu, C., Genest, P., Papadopoulou, B., and Ouellette, M. (2000) Amplification of the ABC transporter gene PGPA and increased trypanothione levels in potassium antimonyl tartrate (SbIII) resistant *Leishmania tarentolae*. *Mol Biochem Parasitol* **108:** 131–135.

Hastings, P.J., Ira, G., and Lupski, J.R. (2009) A microhomology-mediated break-induced replication model for the origin of human copy number variation. *PLoS Genet* **5:** e1000327.

Ivens, A.C., Peacock, C.S., Worthey, E.A., Murphy, L., Aggarwal, G., Berriman, M., *et al*. (2005) The genome of the kinetoplastid parasite, *Leishmania major*. *Science* **309:** 436–442.

Jha, T.K., Sundar, S., Thakur, C.P., Bachmann, P., Karbwang, J., Fischer, C., *et al*. (1999) Miltefosine, an oral agent, for the treatment of Indian visceral leishmaniasis. *N Engl J Med* **341:** 1795–1800.

Krzywinski, M., Schein, J., Birol, I., Connors, J., Gascoyne, R., Horsman, D., *et al*. (2009) Circos: an information aesthetic for comparative genomics. *Genome Res* **19:** 1639–1645.

Kumar, D., Singh, R., Bhandari, V., Kulshrestha, A., Negi, N.S., and Salotra, P. (2012) Biomarkers of antimony resistance: need for expression analysis of multiple genes to

distinguish resistance phenotype in clinical isolates of *Leishmania donovani*. *Parasitol Res* **111:** 223–230.

Lee, N., Bertholet, S., Debrabant, A., Muller, J., Duncan, R., and Nakhasi, H.L. (2002) Programmed cell death in the unicellular protozoan parasite *Leishmania*. *Cell Death Differ* **9:** 53–64.

Legare, D., Richard, D., Mukhopadhyay, R., Stierhof, Y.D., Rosen, B.P., Haimeur, A., *et al*. (2001) The *Leishmania* ATP-binding cassette protein PGPA is an intracellular metal-thiol transporter ATPase. *J Biol Chem* **276:** 26301–26307.

Leprohon, P., Legare, D., Raymond, F., Madore, E., Hardiman, G., Corbeil, J., and Ouellette, M. (2009) Gene expression modulation is associated with gene amplification, supernumerary chromosomes and chromosome loss in antimony-resistant *Leishmania infantum*. *Nucleic Acids Res* **37:** 1387–1399.

Li, H., and Durbin, R. (2010) Fast and accurate long-read alignment with Burrows-Wheeler transform. *Bioinformatics* **26:** 589–595.

Li, H., Ruan, J., and Durbin, R. (2008) Mapping short DNA sequencing reads and calling variants using mapping quality scores. *Genome Res* **18:** 1851–1858.

Li, H., Handsaker, B., Wysoker, A., Fennell, T., Ruan, J., Homer, N., *et al*. (2009) The sequence alignment/map format and SAMtools. *Bioinformatics* **25:** 2078–2079.

Lira, R., Sundar, S., Makharia, A., Kenney, R., Gam, A., Saraiva, E., and Sacks, D. (1999) Evidence that the high incidence of treatment failures in Indian kala-azar is due to the emergence of antimony-resistant strains of *Leishmania donovani*. *J Infect Dis* **180:** 564–567.

Mandal, S., Maharjan, M., Singh, S., Chatterjee, M., and Madhubala, R. (2010) Assessing aquaglyceroporin gene status and expression profile in antimony-susceptible and -resistant clinical isolates of *Leishmania donovani* from India. *J Antimicrob Chemother* **65:** 496–507.

Marquis, N., Gourbal, B., Rosen, B.P., Mukhopadhyay, R., and Ouellette, M. (2005) Modulation in aquaglyceroporin AQP1 gene transcript levels in drug-resistant *Leishmania*. *Mol Microbiol* **57:** 1690–1699.

Mehta, A., and Shaha, C. (2006) Mechanism of metalloid-induced death in *Leishmania* spp.: role of iron, reactive oxygen species, Ca^{2+}, and glutathione. *Free Radic Biol Med* **40:** 1857–1868.

Meltzer, P.S., Guan, X.Y., and Trent, J.M. (1993) Telomere capture stabilizes chromosome breakage. *Nat Genet* **4:** 252–255.

Mittal, M.K., Rai, S., Ravinder, A., Gupta, S., Sundar, S., and Goyal, N. (2007) Characterization of natural antimony resistance in *Leishmania donovani* isolates. *Am J Trop Med Hyg* **76:** 681–688.

Mookerjee Basu, J., Mookerjee, A., Sen, P., Bhaumik, S., Banerjee, S., Naskar, K., *et al*. (2006) Sodium antimony gluconate induces generation of reactive oxygen species and nitric oxide via phosphoinositide 3-kinase and mitogen-activated protein kinase activation in *Leishmania donovani*-infected macrophages. *Antimicrob Agents Chemother* **50:** 1788–1797.

Moreira, W., Leprohon, P., and Ouellette, M. (2011) Tolerance to drug-induced cell death favours the acquisition of multidrug resistance in *Leishmania*. *Cell Death Dis* **2:** e201.

Mukherjee, A., Padmanabhan, P.K., Singh, S., Roy, G., Girard, I., Chatterjee, M., *et al*. (2007) Role of ABC transporter MRPA, gamma-glutamylcysteine synthetase and ornithine decarboxylase in natural antimony-resistant isolates of *Leishmania donovani*. *J Antimicrob Chemother* **59:** 204–211.

Mukherjee, A., Roy, G., Guimond, C., and Ouellette, M. (2009) The gamma-glutamylcysteine synthetase gene of *Leishmania* is essential and involved in response to oxidants. *Mol Microbiol* **74:** 914–927.

Mukherjee, A., Langston, L.D., and Ouellette, M. (2011) Intrachromosomal tandem duplication and repeat expansion during attempts to inactivate the subtelomeric essential gene GSH1 in *Leishmania*. *Nucleic Acids Res* **39:** 7499–7511.

Narayanan, V., Mieczkowski, P.A., Kim, H.M., Petes, T.D., and Lobachev, K.S. (2006) The pattern of gene amplification is determined by the chromosomal location of hairpin-capped breaks. *Cell* **125:** 1283–1296.

Ouellette, M., Fase-Fowler, F., and Borst, P. (1990) The amplified H circle of methotrexate-resistant leishmania tarentolae contains a novel P-glycoprotein gene. *EMBO J* **9:** 1027–1033.

Ouellette, M., Hettema, E., Wust, D., Fase-Fowler, F., and Borst, P. (1991) Direct and inverted DNA repeats associated with P-glycoprotein gene amplification in drug resistant *Leishmania*. *EMBO J* **10:** 1009–1016.

Pal, S., Dolai, S., Yadav, R.K., and Adak, S. (2010) Ascorbate peroxidase from *Leishmania major* controls the virulence of infective stage of promastigotes by regulating oxidative stress. *PLoS ONE* **5:** e11271.

Palatnik-de-Sousa, C.B. (2008) Vaccines for leishmaniasis in the fore coming 25 years. *Vaccine* **26:** 1709–1724.

Papadopoulou, B., Roy, G., and Ouellette, M. (1992) A novel antifolate resistance gene on the amplified H circle of *Leishmania*. *EMBO J* **11:** 3601–3608.

Polakova, S., Blume, C., Zarate, J.A., Mentel, M., Jorck-Ramberg, D., Stenderup, J., and Piskur, J. (2009) Formation of new chromosomes as a virulence mechanism in yeast *Candida glabrata*. *Proc Natl Acad Sci USA* **106:** 2688–2693.

Richard, D., Leprohon, P., Drummelsmith, J., and Ouellette, M. (2004) Growth phase regulation of the main folate transporter of *Leishmania infantum* and its role in methotrexate resistance. *J Biol Chem* **279:** 54494–54501.

Roberts, W.L., Berman, J.D., and Rainey, P.M. (1995) *In vitro* antileishmanial properties of tri- and pentavalent antimonial preparations. *Antimicrob Agents Chemother* **39:** 1234–1239.

Rogers, M.B., Hilley, J.D., Dickens, N.J., Wilkes, J., Bates, P.A., Depledge, D.P., *et al*. (2011) Chromosome and gene copy number variation allow major structural change between species and strains of *Leishmania*. *Genome Res* **21:** 2129–2142.

Sambrook, J., Fritsch, E.F., and Maniatis, T. (1989) *Molecular Cloning*. New York: Cold Spring Harbour laboratory.

Selmecki, A., Forche, A., and Berman, J. (2006) Aneuploidy and isochromosome formation in drug-resistant *Candida albicans*. *Science* **313:** 367–370.

Sereno, D., Cavaleyra, M., Zemzoumi, K., Maquaire, S., Ouaissi, A., and Lemesre, J.L. (1998) Axenically grown

amastigotes of *Leishmania infantum* used as an *in vitro* model to investigate the pentavalent antimony mode of action. *Antimicrob Agents Chemother* **42:** 3097–3102.
Sereno, D., Holzmuller, P., Mangot, I., Cuny, G., Ouaissi, A., and Lemesre, J.L. (2001) Antimonial-mediated DNA fragmentation in *Leishmania infantum* amastigotes. *Antimicrob Agents Chemother* **45:** 2064–2069.
Shaked-Mishan, P., Ulrich, N., Ephros, M., and Zilberstein, D. (2001) Novel Intracellular SbV reducing activity correlates with antimony susceptibility in *Leishmania donovani*. *J Biol Chem* **276:** 3971–3976.
Smyth, G.K. (2004) Linear models and empirical bayes methods for assessing differential expression in microarray experiments. *Stat Appl Genet Mol Biol* **3:** Article3.
Smyth, G.K., and Speed, T. (2003) Normalization of cDNA microarray data. *Methods* **31:** 265–273.
Smyth, G.K., Michaud, J., and Scott, H.S. (2005) Use of within-array replicate spots for assessing differential expression in microarray experiments. *Bioinformatics* **21:** 2067–2075.
Sudhandiran, G., and Shaha, C. (2003) Antimonial-induced increase in intracellular Ca^{2+} through non-selective cation channels in the host and the parasite is responsible for apoptosis of intracellular *Leishmania donovani* amastigotes. *J Biol Chem* **278:** 25120–25132.
Sundar, S. (2001) Drug resistance in Indian visceral leishmaniasis. *Trop Med Int Health* **6:** 849–854.
Tamar, S., and Papadopoulou, B. (2001) A telomere-mediated chromosome fragmentation approach to assess mitotic stability and ploidy alterations of *Leishmania* chromosomes. *J Biol Chem* **276:** 11662–11673.
Ubeda, J.M., Legare, D., Raymond, F., Ouameur, A.A., Boisvert, S., Rigault, P., *et al*. (2008) Modulation of gene expression in drug resistant *Leishmania* is associated with gene amplification, gene deletion and chromosome aneuploidy. *Genome Biol* **9:** R115.
Vergnes, B., Gourbal, B., Girard, I., Sundar, S., Drummelsmith, J., and Ouellette, M. (2007) A proteomics screen implicates HSP83 and a small kinetoplastid calpain-related protein in drug resistance in *Leishmania donovani* clinical field isolates by modulating drug-induced programmed cell death. *Mol Cell Proteomics* **6:** 88–101.
Wilkie, A.O., Lamb, J., Harris, P.C., Finney, R.D., and Higgs, D.R. (1990) A truncated human chromosome 16 associated with alpha thalassaemia is stabilized by addition of telomeric repeat (TTAGGG)n. *Nature* **346:** 868–871.
Wyllie, S., Vickers, T.J., and Fairlamb, A.H. (2008) Roles of trypanothione S-transferase and tryparedoxin peroxidase in resistance to antimonials. *Antimicrob Agents Chemother* **52:** 1359–1365.
Wyllie, S., Mandal, G., Singh, N., Sundar, S., Fairlamb, A.H., and Chatterjee, M. (2010) Elevated levels of tryparedoxin peroxidase in antimony unresponsive *Leishmania donovani* field isolates. *Mol Biochem Parasitol* **173:** 162–164.
Yatsenko, S.A., Brundage, E.K., Roney, E.K., Cheung, S.W., Chinault, A.C., and Lupski, J.R. (2009) Molecular mechanisms for subtelomeric rearrangements associated with the 9q34.3 microdeletion syndrome. *Hum Mol Genet* **18:** 1924–1936.

Supporting information

Additional supporting information may be found in the online version of this article at the publisher's web-site.